Adamantane as a Probe for Studies of Spin Clustering with Multiple Quantum NMR

G. Buntkowsky,*,† E. Roessler,‡ M. Taupitz,§ and H. M. Vieth§

Institut für organische Chemie and Institut für Experimentalphysik, Freie Universität Berlin, 14195 Berlin, Germany, and Physikalisches Institut, Universität Bayreuth, 95440 Bayreuth, Germany

Received: April 1, 1996; In Final Form: June 12, 1996[⊗]

Time domain ^{1}H multiple quantum NMR (MQ NMR) was applied to study binary guest/host systems. We investigated protonated adamantane-h_{16} (A-h_{16}) molecules in deuterated crystalline adamantane-d_{16} (A-d_{16}) and in glassy polystyrene-d_8 (PS) for various guest concentrations and coupling times τ/τ_c. For pure A-h_{16} crystals spin clusters of more than 1000 connected spins were observed. We observed the evolution of the multiple quantum connectivities as a function of the coupling time. In all cases the growth curves of the multiple quantum orders can be described by a master curve, showing the validity of a scaling law. For the diluted systems the master curve is obtained by multiplying the time axis with the square root of the dipolar line width $(\Delta\nu)^{1/2}$. The different local structure of the systems leads to characteristic growth curves, in particular to a quadratic function for the crystalline and to a linear function for the glassy material. For short coupling times these differences can be attributed to geometrical constraints caused by the polymer chains while for longer coupling times geometrical constraints and dynamics of the polymer chains can both be responsible for the different growth curves. The technique was applied to study slow phase separation processes in a solution of A-h_{16} in PS.

1. Introduction

Information on the spatial distribution of molecules in a given state of aggregation is primarily obtained from scattering experiments. In recent years substantial progress has been made by nuclear magnetic resonance (NMR) spectroscopy to unravel the configuration of molecules, in particular of proteins in solution. The pioneering work of Pines and collaborators[1−3] has demonstrated that multiple quantum (MQ) NMR[4−9] provides a tool to investigate the spatial distribution of spins also in the solid state. The dipolar interaction between the spins varies as $1/R_{ij}^3$ with the distance R_{ij} between the spin i and j and is therefore very sensitive to the distance of the spins. In most cases protons were studied, mainly because of their high gyromagnetic ratio. Special pulse sequences have been designed to selectively study the evolution of dipolar interaction within the local environment of a given spin by controlling the effective contact time. From this network of dipolar couplings, information about the spatial distribution of spins can be extracted. For example, MQ NMR studies have demonstrated a nonstatistical distribution of hydrogen in amorphous silicon.[2]

The accuracy of such structural results is reduced if contributions of strong intramolecular homonuclear dipolar interactions are present. In such cases a reliable method is needed to separate intra- and intermolecular parts in the MQ spectra. This is often not feasible without assumptions of a structural model. Thus the sensitivity with respect to the spatial configuration of the molecules is highest if all intramolecular couplings in the samples are suppressed. One efficient approach is to use a molecule which performs a sufficiently fast motional process such that all intramolecular dipole couplings are averaged to zero and therefore to get signals only from intermolecular clustering. As a well-known example the molecule adamantane ($C_{10}H_6$) fulfills this condition.[10] Due to a fast tetrahedral jump process all intramolecular dipole interaction is sufficiently suppressed at room temperature. Moreover, the high mobility of the adamantane reduces also the rate of relaxational processes among the protons, which would otherwise disturb the development and the observation of high order coherences. Accordingly, adamantane is well suited to probe connections among distant spins and to observe large intermolecular spin clusters.

This allows in particular to monitor in detail the evolution of dipolar couplings in crystals and to check basic assumptions usually made in analyzing MQ spectra. In recent studies it has been shown,[11] that on the one hand the development of the MQ coherences shows characteristic features which can be correlated to the particular geometrical structure of the spin clusters. On the other hand, for all geometrically similar arrangements a common master curve for the dependence of the effective cluster size on the coupling time has been found. Following this line we investigated to what extent the different degree of geometrical order in crystalline and glassy systems is reflected in the evolution of the multiple quantum coherences.

As an application we show that MQ NMR allows the investigation of slow phase separation processes on the molecular level in binary systems. For demonstration the segregation in an adamantane/polymer system is studied under conditions of cyclic tempering.

We start with a well-blended mixture and can assume that the adamantane molecules are homogeneously distributed in the polymer matrix. In the course of the tempering process this homogeneous system changes and an adamantane-enriched phase together with an adamantane-depleted polymer phase is formed. Multiple quantum NMR is sensitive for numbers of coupled spins in the range of 10^2-10^3 and below, which allows the investigation of the early[12−15] stages of phase separation, which are only poorly accessible by electron and optical microscopy and scattering methods.

A requirement for such a study is the investigation of mixed isotopic systems, because it relates the size of spin cluster to the concentration of the guest molecules in the solid. Such information is needed to evaluate the concentration of each phase during phase separation. Accordingly, our article starts with a

† Institut für organische Chemie, Freie Universität Berlin.
‡ Universität Bayreuth.
§ Institut für Experimentalphysik, Freie Universität Berlin.
⊗ Abstract published in *Advance ACS Abstracts,* December 1, 1996.

S1089-5639(96)00963-2 CCC: $14.00

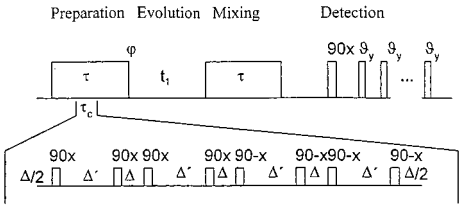

Figure 1. Standard multiple quantum pulse sequence for spin counting with multiple quantum NMR. The preparation and evolution time propagators are built from basic 8-pulse blocks with duration τ_c shown in the lower part of the figure. Detection of the magnetization is done with a pulsed spin locking sequence.

brief summary of the necessary principles of MQ-NMR in solids; then a few novel features of our home-made NMR spectrometer used for the MQ investigations are described. In the main part of the article we present experiments of isotopically mixed adamantane and of adamantane in polystyrene.

2. Multiple Quantum NMR

The basic principle behind multiple quantum NMR is that an isolated group of N nuclear spins can absorb only a finite number of rf quanta[16] at a single moment, which is related to *N*. This feature is based on the fact that the individual spins become correlated with one another by virtue of their dipolar couplings and show collective behavior as a group of spins. To establish this collective motion, the spins need time to communicate on the order of the inverse of the size of their mutual coupling. Since the dipolar interaction between spins is proportional to the inverse cube of their distance, spins with a greater distance need more time to communicate than spins separated by a smaller distance.

In an infinite spin system with a statistical distribution of the individual spins, the number of correlated spins is a monotonically growing function of the coupling time τ_c, whereas in the case of well-separated spin clusters, the number of coupled spins will be limited to the number of spins in one cluster.[17] Only for very long coupling times a correlation between spins from different clusters is expected, leading eventually to an infinite number of correlated spins. By changing the coupling time in the multiple quantum experiment, it is therefore possible to map out the size distribution in the spin system and to distinguish between a clustered or a statistical behavior.

For optimum sensitivity for cluster detection we used phase-incremented (PI) MQ-NMR.[18,19] The basic pulse sequence is shown in Figure 1. It is subdivided into the preparation (τ), evolution (t_1), mixing (τ), and detection (t_2) period. During the preparation time the multiple quantum coherences are created. The pulse sequence applied during the preparation period, which consists of a series of eight pulses, is shown in the lower part of Figure 1. This pulse train leads to an average dipolar Hamiltonian of the form[20,21]

$$H_D = {}^1/_2 \sum_{j<k} D_{jk} (I_{j+}I_{k+} + I_{j-}I_{k-}) \qquad (1)$$

where the D_{jk} are the dipolar coupling between spins *i* and *j* and the I_{j+} and I_{j-} are the usual spin raising and lowering operators. Since H_D is a sum of products of the type $I_{j+}I_{k+}$, which are pure double quantum operators (i.e., only states with $|\Delta M| = 2$ are coupled), only even multiple quantum coherences can be created during the preparation period. During the evolution time, the multiple quantum coherences evolve freely under the full, not averaged, Hamiltonian.

In the PI experiment, the rf-phase difference φ between the pulses in the preparation and mixing sequence is incremented, while the evolution time t_1 is kept constant. The consequence is that all multiple quantum lines of one order will appear integrated at the same position in the spectrum, therefore giving a better signal to noise ratio as compared to pulse sequences which allow spectral resolution. During the mixing period the multiple quantum coherences are converted into observable Zeeman magnetization. The pulse sequence during the mixing period is identical to the sequence during the preparation period, except that all pulses are phase shifted with respect to the initial pulses. In particular, a phase shift of 90° leads to the so-called time reversal,[18] which causes all coherences to have the same phase at the end of the mixing period. For optimum sensitivity the detection of the NMR signal is done by a standard pulsed spin locking sequence.[22] In a pointwise manner the initial amplitude of this spin lock signal is recorded as a function of the phase shift φ between preparation and mixing sequence. This mapping is called, in analogy to normal NMR, the multiple quantum FID, which after Fourier transformation gives the multiple quantum spectrum. Since the signal is strictly periodic in 2π, it is sufficient to vary φ over this range. To increase the spectral resolution the data can afterwards be extended over a wider phase range[18] by adding several multiple quantum FIDs in a consecutive manner. The highest observable coherence order N_{max} is determined by the phase increment $\Delta\varphi$:

$$N_{max} = \pi/\Delta\varphi \qquad (2)$$

A detailed numerical analysis for the behavior of smaller spin systems can be found in ref 24. For larger spin systems ($N > 6$) the number of coupled spins can in good approximation be determined from the width of the multiple quantum spectra[3] by assuming a Gaussian line shape of the multiple quantum spectra,

$$I(n) = I_0 \exp(-n^2/2\sigma^2) \qquad (3)$$

N is given as

$$N = 2\sigma^2 \qquad (4)$$

An easy way to interpret this equation is by counting the number of transitions in the different multiple quantum orders Z_n and approximating the resulting combinatorial term using Stirling's formula:

$$Z_n = \binom{2N}{N+n} \approx \frac{4^N}{\sqrt{N\pi}} \exp\left(-\frac{n^2}{N}\right) \qquad (5)$$

A more detailed derivation of eq 3 is given in ref 24, where the development of multiple quantum coherences is calculated on the basis of a hopping model. An important result of these theoretical studies is that the evolution of multiple quantum dynamics is determined by rate constants $\Gamma_{Kn;K\pm1,n\pm2}$ which can be factorized into a term describing the geometric structure of the spin system, S_1, which is the same for all rates and into a second term $W_{Kn;K\pm1,n\pm2}$ describing the connectivity of different states $|Kn\rangle$ in the Liouville space (i.e., coherences) due to the selectivity of the Hamiltonian.

$$\Gamma_{Kn;K\pm1,n\pm2} = W_{Kn;K\pm1,n\pm2} S_1 \qquad (6)$$

The structural factor S_1 characterizes the average dipolar interaction,[24] which originates from the spatial distribution of the spins. S_1 behaves as a scaling factor and can be further factorized into two components, one which is characteristic for the mean distance between the spins, i.e., their concentration, and one which is characteristic for the geometrical arrangement of the spins. Thus the evolution of the MQ orders can be scaled

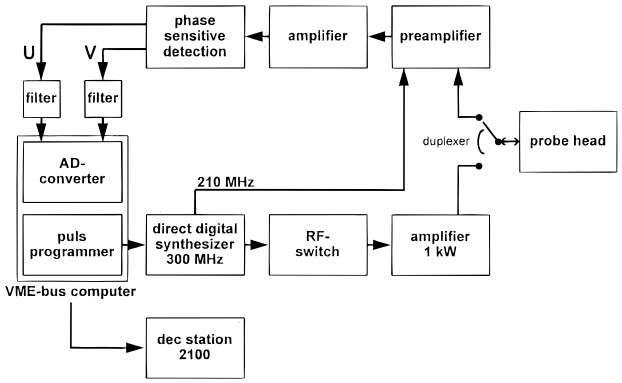

Figure 2. Schematic view of the experimental setup.

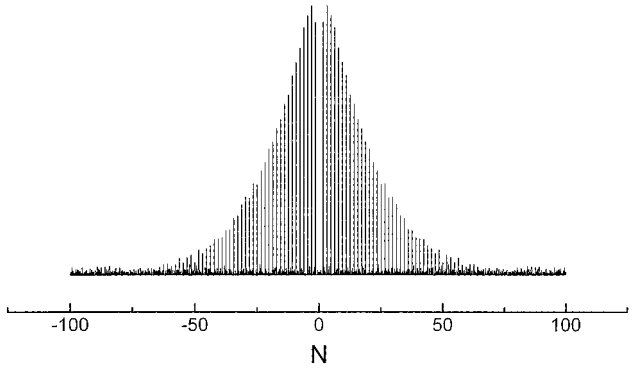

Figure 3. Multiple quantum spectrum of pure adamantane-h_{16} for a coupling time of $\tau/\tau_c = 12$. This spectrum displays more than 1000 correlated proton spins.

to a concentration-independent master curve for spins in a similar geometry. A detailed discussion in ref 11 shows that the square root of Van Vleck's second moment, $M_2^{1/2}$, is an appropriate choice for the scaling.

$$S_1 \approx M_2^{1/2} = [{}^3/_5\gamma^4\hbar^2 I(I+1)\sum_{jk} r_{jk}^{-6}]^{1/2} \qquad (7)$$

The discussion on the scaling factors in ref 11 is based on the assumption that the second moment of the line is dominated by the homonuclear dipolar interaction of the spins observed in the MQ-NMR experiment. While this is in general true for abundant ^{1}H or ^{19}F spin systems, it is not the case for isotopically highly diluted systems as in our experiments. In our case the NMR line width is strongly affected by the heteronuclear dipolar interaction with neighboring deuterons. As a consequence, we cannot directly use the second moment of the NMR line as a measure of the scaling factor but have first to deconvolute the line with respect to such heteronuclear contributions. To do so, we can use the well-known concentration dependence of the dipolar line width to estimate the homonuclear dipolar contribution to the width of the NMR line. For diluted spin systems the concentration c is related to the second moment M_2 and the dipolar line width by[25]

$$c \propto M_2/M_4^{1/2} \propto \Delta\nu \qquad (8)$$

If the fourth moment $M_4(c)$ shows only a slight variation upon changing of the concentration, we can approximate eq 8 by a proportionality between concentration and second moment. This linearization is justified by the calculations shown in ref 26. Thus, one obtains that for diluted systems the scaling factor $M_2^{1/2}$ is proportional to $\Delta\nu^{1/2}$

$$M_2^{1/2} \propto \Delta\nu^{1/2} \qquad (9)$$

Alternatively, a scaling with an average dipolar coupling $\langle D\rangle$ is proposed in ref 11, which is related to the second moment by a structural factor f_c:

$$\langle D\rangle = \frac{2}{3}\left(\frac{M_2}{f_c}\right)^{1/2} \qquad (10)$$

From the resulting master curve the characteristic geometrical information can be extracted.

3. Experimental Setup

3.1. The Spectrometer. A scheme of our experimental setup is shown in Figure 2. A major experimental problem of the technique described above is the stringent requirements for the accuracy of the generated phase shifts and the B_1 field homogeneity of the rf pulses to generate the average Hamiltonian of eq 1. As mentioned in the previous section, the multiple quantum spectrum is calculated by Fourier transforming the multiple quantum FID, which is measured in a pointwise manner by a stepwise increase of the phase. Errors in the phase shifts can lead to artificial periodicities in the multiple quantum FID which significantly distort the line shape of the multiple quantum spectrum, in particular in the wings of the line, where the high-order coherences are observed. For optimum performance we compared two different techniques to generate the phase shifts, (i) a digitally controlled phase shifter (DAICO) in combination with a feedback circuit for stabilizing the rf amplitude and (ii) a synthesizer with digital phase control (PTS310). Both devices were controlled by a pulse programmer with a 100 ns resolution, 32-bit binary output, and 32K maximum pulse program length. The digital-controlled synthesizer showed a far superior performance, and therefore all actual experiments were done with the digital synthesizer. After the synthesizer, the actual pulses were generated with a fast rf switch (10 ns rise time). The width of the 90° pulse was 3.6 μs and the exact 90° condition for the pulses was adjusted by control of the rf level. The cycle time τ_c in the pulse sequence was 64 μs. To suppress artifacts due to B_1 field inhomogeneity we used a solenoid coil with variable pitch angle with a residual B_1 inhomogeneity below 2.3% over the sample volume.[27] With this setup we could easily observe cluster sizes of more than 1000 coupled spins in solid adamantane (see Figure 3) with only minor distortions of the spectrum.

3.2. Samples and Preparation. Six different samples were prepared and sealed in glass tubes with an outer diameter of 5 mm (all concentrations are given in weight percent): (1) neat crystalline adamantane with natural isotope abundance; isotopically mixed samples of protonated adamantane (A-h_{16}) in fully deuterated adamantane (A-d_{16}, degree of deuteration > 98%) with concentrations of (2) 2.4%, (3) 5.4%, (4) 12.4%; solutions of (A-h_{16}) in fully deuterated polystyrene-d_8 (PS, MW 80 000, degree of deuteration > 99%) with A-h_{16} concentrations of (5) 6.3% and (6) 12.0%. The crystalline samples were mechanically mixed and filled into the tubes. The tubes were evacuated and sealed. The crystalline samples were melted several times (T > 170 °C) to assure complete mixing. The preparation of the polymer samples was done in the following way: Before mixing, the polystyrene was degassed for about 5 days at a temperature close to the glass transition (T = 103 °C). Then the adamantane was added and the tubes were sealed. The polymeric samples were tempered for 5 days at T = 140 °C which is well above the glass transition (T_g = 104 °C) to completely dissolve the adamantane and then rapidly cooled to room temperature to avoid phase separation. In the phase

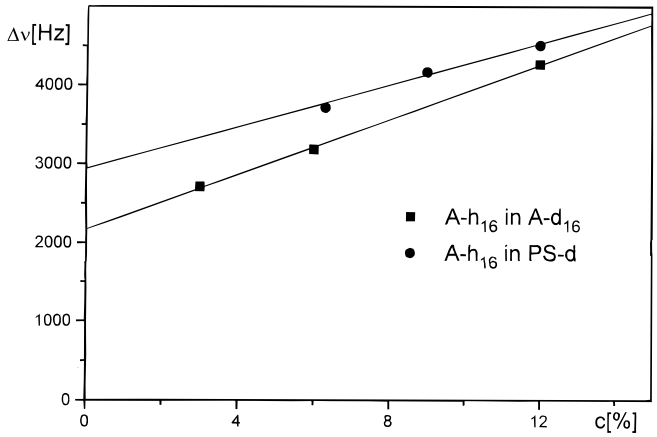

Figure 4. NMR line width $\Delta\nu_{1/2}$ as a function of the adamantane concentration (c) in the deuterated polystyrene matrix (upper curve) and in the deuterated adamantane matrix (lower curve). The symbols mark the experimentally determined line width (fwhh) and the solid line is the result of a linear fit to these data. The value extrapolated for $c = 0$ is the residual line width without contributions from homonuclear dipolar interaction among the protons.

separation experiments the samples were tempered at 103 °C for the specified time and than rapidly cooled down to room temperature to stop further phase separation. All samples had a spherical shape with a diameter of about 4.5 mm.

4. Results and Discussion

In all our experiments the multiple quantum spectra showed good agreement with the predicted Gaussian envelope of eq 3. Only when increasing the contact time to values corresponding to very large spin systems ($N \gg 100$) did we observe growing deviations from the Gaussian shape, leading to a line shape resembling more a Lorentzian line, with wider wings and more intensity in the center than a Gaussian. Such deviations from a Gaussian shape have also been reported by other authors[28,29] and were attributed to a nonstatistical behavior of higher order correlations, so that the basic assumptions of eqs 3 and 5 are not fully valid at these high correlations. Following the approach of these authors we used a Gaussian line as an approximation to the line shape for all spectra, which allowed us to use the simple relationship of eq 3 between the number of coupled spins and the line width for all coupling times.

4.1. Multiple Quantum Spectra. In a first step conventional solid state NMR experiments were performed to obtain the magnetic parameters necessary for the analysis of multiple quantum spectra. One particular purpose was to separate the homo- and heteronuclear parts of the dipolar line width. In addition we wanted to test whether any indications of a nonstatistical distribution of the adamantane in the polystyrene are observable in the NMR spectrum. Therefore, we recorded the NMR spectra of the samples as a function of the A-h_{16} concentration. For both the crystalline and the polymeric matrix we found, in good approximation, a linear dependence of the line width on the concentration. This is the expected result for diluted spin systems, where the dipolar line width is proportional to the concentration.[25] From this concentration dependence the homonuclear dipolar parts of the line width are easily determined and can be used to scale the individual experimental curves. The results are shown in Figure 4. By extrapolating to zero concentration of A-h_{16} (infinite dilution), the residual width of the adamantane line was determined, which is caused by interactions other than homonuclear dipole coupling among the adamantane protons. The values were 2.34 kHz for the isotopically mixed adamantane system and 2.87 kHz for the

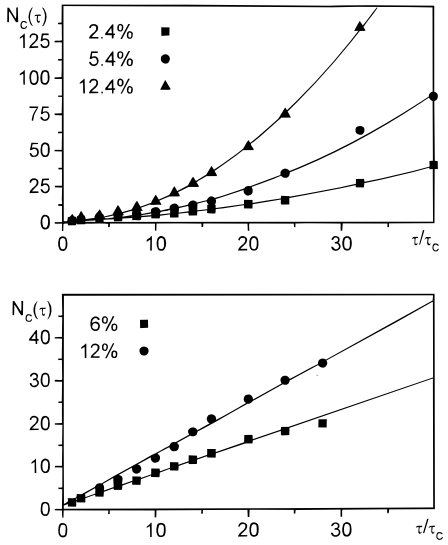

Figure 5. Number of correlated spins as a function of the coupling time for three different concentrations of crystalline system adamantane-h_{16} in adamantane-d_{16} (upper panel) and the number of correlated spins as a function of the coupling time for admantane-h_{16} as guest in a fully deuterated polystyrene host glass (lower panel). The monotonic increase of the curves shows that there is no direct clustering of the admantane molecules in the host, which would be visible in a flat part of the curve. Note the different growth curves for the glassy polymer system compared to the crystalline system.

adamantane/polystyrene system. The difference between these values and the total line width was taken as the homonuclear dipolar line broadening due to interaction between protonated adamantane molecules. Furthermore, using eq 8 we can conclude from the linear relationship between line width and adamantane concentration that in the polymer samples the adamantane fulfills the condition of high dilution with statistical distribution in the polystyrene host. This conclusion is supported by the fact that the measured line widths are close to the line widths of the isotopically mixed systems. We take this as evidence that the reorientation dynamics of the adamantane molecules is still fast enough to average out the intramolecular dipolar interactions and that on average the distances between different protonated adamantane molecules are comparable for both types of systems. After this, initial multiple quantum NMR measurements were carried out to determine the number of coupled spins $n(\tau)$ as a function of the coupling time τ for both systems. The upper diagram of Figure 5 shows the results for crystalline adamantane with different concentrations of A-h_{16}. As expected, the number of coupled spins grows monotonically with the coupling time τ and the rate of growth increases with increasing concentration of the protonated molecules. These results are similar to measurements of protonated hexamethylbenzene in deuterated hexamethylbenzene.[28] The solid lines mark the results of an extrapolation of the data, which is discussed in further detail below. The lower part of Figure 5 shows the corresponding results for adamantane in deuterated polystyrene at different concentrations directly after sample preparation. There are no indications of a nonstatistical clustering of the adamantane molecules, which would be indicated by a flat part of the curves for intermediate τ values.

Figure 6 compares the growth curves of the adamantane/polystyrene system with the curves of the A-h_{16} in deuterated adamantane at equivalent adamantane concentrations. For short coupling times the effective cluster size grows faster in the adamantane/polystyrene system. This effect is particularly pronounced in the 12% A-h_{16} systems for $\tau/\tau_c < 20$. For further analysis the following results are of particular importance: (i)

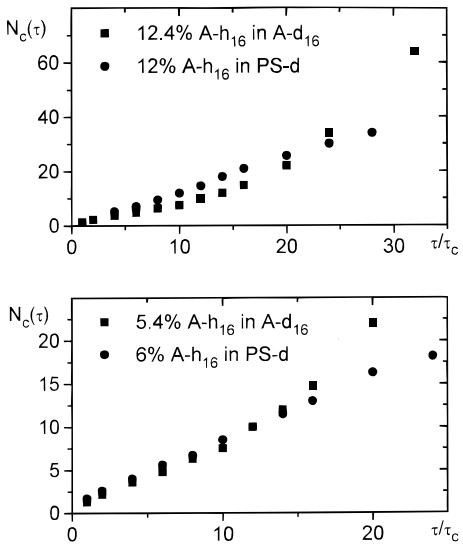

Figure 6. Multiple quantum growth curves of the adamantane/polystyrene system compared to the curves of the A-h_{16} in deuterated adamantane at equivalent adamantane concentrations for short coupling times. Note that for short values of τ/τ_c the effective cluster size grows faster in the polymer system.

the isotropic reorientation of the adamantane molecule is still fast enough to average out intramolecular dipolar interactions among the adamantane protons, which was a necessary condition for using it as a probe for intermolecular clustering and (ii) after the initial preparation of the sample the adamantane guests have a statistical distribution in the glassy polystyrene host matrix. As was discussed above, for bulk spin systems the growth of the multiple quantum orders as a function of the coupling time can be described by a master curve, the shape of which is characteristic for each type of system when scaling the individual curves with the dipolar line width. One intention of our study was to see whether this scaling behavior is also true for diluted systems, which no longer have a regular arrangement of the spins, when a scaling factor determined from the concentration dependence of the homonuclear part of the NMR line width is used. For reasons discussed in detail below, we tried two different scaling factors on the three different concentrations of A-h_{16} in A-d_{16}. The upper diagram in Figure 7 shows a scaling of the data with their homonuclear dipolar line width (i.e., $\Delta\nu$) obtained from Figure 4 by multiplying the coupling times with $\Delta\nu$. This scaling corresponds to the scaling done in previous works on systems of abundant spins.[11] The lower diagram in Figure 7, however, shows a scaling of the data with the square root of their homonuclear dipolar line (i.e., $\Delta\nu^{1/2}$) by multiplying the coupling times with $(\Delta\nu)^{1/2}$. As can be seen, the latter scaling gives a far better result and all curves coincide to one single master curve after the scaling. The solid line is the result of a parabolic fit of the experimental data, which was used by other authors[11] as an empirical function to describe the evolution of multiple quantum orders in samples with a crystalline structure. As can be seen, the curves interpolate well the experimental data. This interpolation, however, is not unique; another empirical function used by the same authors to describe these types curves is $\exp(\alpha\sqrt{\tau})$, which approximates the curves equally well. Due to its simplicity, we will use the parabolic approximation as the experimental master curve for the crystalline system. The curves for the glassy system were scaled in an identical manner (Figure 8). Again the scaling with $(\Delta\nu)^{1/2}$ is superior to the scaling with $(\Delta\nu)$. Thus the scaling is also valid in the case of the glassy system. The solid line shows the resulting master curve. This curve exhibits an

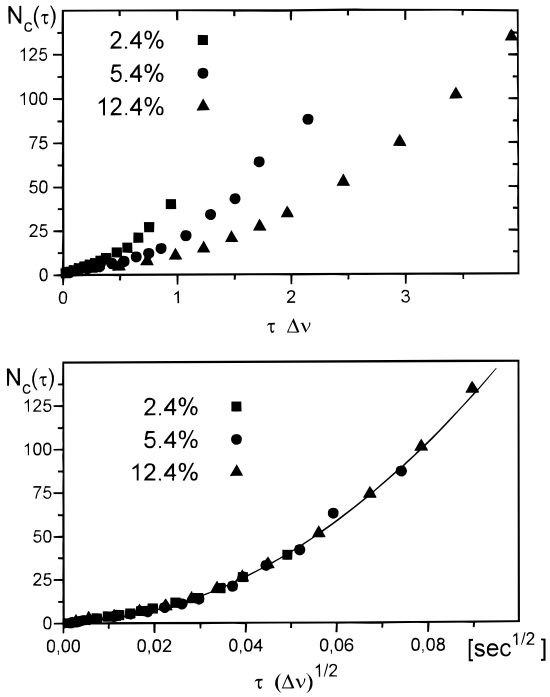

Figure 7. Master curve for crystalline admantane. The curves of Figure 5 were scaled with the homonuclear dipolar line width of the NMR spectrum by multiplying τ with $\Delta\nu$ (upper panel) and by multiplying τ with $(\Delta\nu)^{1/2}$ (lower panel). Only the latter scaling gives a common master curve for all three concentrations. The solid line shows a parabolic fit to these scaled data, which reproduces well the characteristic growth curve.

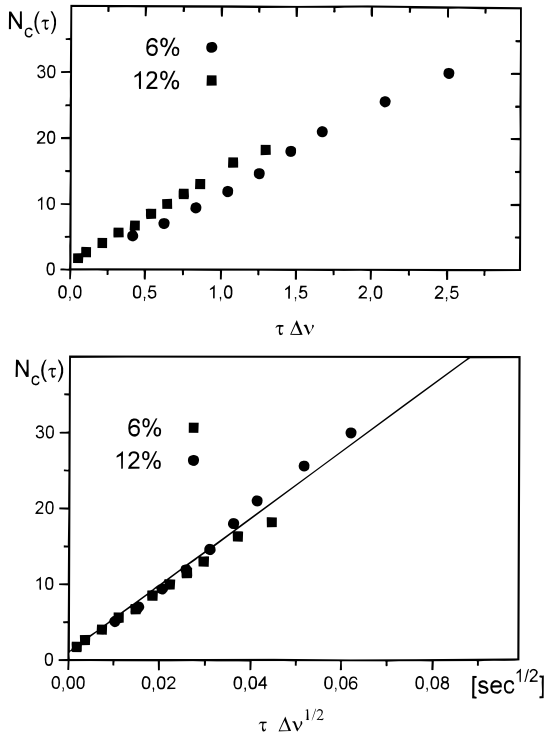

Figure 8. Master curve for the glassy system adamantane in polystyrene. The curves of Figure 5 were scaled with the dipolar line width of the NMR spectrum by multiplying τ with $\Delta\nu$ (upper panel) and by multiplying τ with $(\Delta\nu)^{1/2}$ (lower panel). The solid line shows a linear fit to the data scaled with $(\Delta\nu)^{1/2}$.

interesting difference, compared to the previous results: In contrast to the parabolic behavior of the crystalline system in Figure 7, there is a linear relation between the number of coupled spins $n(\tau)$ and the coupling time τ for the glassy polymer system

(Figure 8). In the following we discuss these scaling factors. The experimental result is that for the investigated dilution range, these curves can be scaled to one common master curve by using the $(\Delta\nu)^{1/2}$ scaling. We wish to note that instead of using the $(\Delta\nu)^{1/2}$ as a scaling factor, because of the linear dependence of $\Delta\nu$ on the concentration c shown in Figure 4, $c^{1/2}$ can also be used as a scaling factor. However, we prefer the scaling with $(\Delta\nu)^{1/2}$, because it allows to relate two different quantities accessible by NMR methods.

As mentioned above, for abundant spin systems, the scaling with $M_2^{1/2}$ or alternatively with an averaged dipolar coupling $\langle D\rangle$ allows a scaling of different multiple quantum growth curves to one single master curve.[11] In the systems investigated here, however, there is a dilute statistical distribution of protonated guest molecules in the host matrices. In this situation it is not possible to simply introduce a geometric structure factor which explains the scaling factor, because there exists no regular lattice of the protonated guest molecules. This situation resembles the case of the dipolar line broadening in magnetically diluted systems, which was discussed in ref 25 and which is referred to above (eqs 8 and 9), where a change of the dependence of the dipolar line width on the dilution factor from a square root behavior to a linear behavior is observed, resulting from line changes in the NMR line.

Assuming for simplicity the fcc structure of the adamantane,[31] one molecule has 12 nearest neighbors. Concentrations of protonated adamantane between 3% and 12% were used. At a concentration of 3% the majority of the protonated adamantane molecules will have no direct protonated neighbor and have to establish the dipolar couplings over two lattice distances. However, there are some molecules which will have a direct neighbor and which will therefore exhibit a much faster growth as compared to the single molecules. By increasing the concentration the number of molecules with a protonated neighbor is increased, until for example in the 12% case in average every protonated molecule will have at least one protonated neighbor and also a substantial probability for two protonated neighbors. Thus a complicated superposition of growth curves from molecules with different numbers of protonated neighbors occurs. For high concentrations close to 100% these curves will finally approach the master curve described for abundant systems.[11] We wish to note that it would be interesting to investigate the concentration dependence between 10% and 100% to observe these changes in the master curves.

Next we want to discuss the differences in the shapes of the master curves of the crystalline versus the polymer system. Since the rather narrow ^{1}H NMR lines of both dilute systems have about the same width, we assume that we can exclude relaxation effects caused by a different mobility of the adamantane guest molecules as the origin of the different master curves. Instead, two other possible explanations for the different types of master curve exist: (1) dynamically, due to the mobility of the polymer matrix, or (2) statically, due to structural factors from different arrangements of the guest molecules in the host matrix. In the rest of this section we want to discuss these two cases in more detail:

The first explanation of the differences in the master curve is dynamic effects caused by the mobility of the polymer matrix. As has been pointed out by ref 32, molecular dynamics in a host can severely hinder the refocusing of the multiple quantum coherences between the guest molecules. This effect will be more pronounced for high coherence orders, because more spins are involved in these high-order coherences; i.e., there is a short phase relaxation (T_2) time of these coherences. Thus, a smaller effective cluster size is measured at longer coupling times. In general, dynamic process in a polymer, such as chain movements, will be on a faster time scale than dynamic processes in a crystal. Thus, for short coupling times, where only a few molecules are involved in creating the coherences, similar growth curves are expected at the same concentration, while at higher coupling times the growth curves of the glass will be below the curve of the crystal. Comparing this with the experimental finding that at the same concentration of protonated guest molecules for short coupling times the number of coupled spins grows faster in the polymer than in the crystal, one can exclude this explanation for short coupling times. For long coupling times this mobility could explain the observed differences in the master curves of the glassy versus crystalline system; however, T_1 relaxation measurements[33] on the same system indicate that there is only a very low mobility of the polystyrene molecules in the matrix. A final experimental proof of this explanation would be a measurement of the temperature dependence of the cluster size.

Qualitatively, the structural differences between glassy and crystalline systems have the following consequences: In the numerical calculations of ref 30 it was shown that for crystalline systems the characteristic dipolar coupling responsible for multiple quantum coherences is the coupling among nearest neighbors in the crystal. With this approximation it was possible to reduce the large coupling networks in the full dipolar Hamiltonian of eq 1 to a much simpler type of coupling scheme by using only the coupling among such neighbors. Applying this method to a crystal results in a small number of possible coupling constants, due to the regular structure of the crystal lattice. In contrast, there are two basic differences in the polymer system: (i) there is no regular lattice in the glassy polymer and therefore a much broader distribution of nearest-neighbor distances is expected and (ii) the shape of the glass-forming polystyrene molecule itself leads to geometrical constraints for the possible positions of guest molecules. When looking at one monomeric styrene unit, at least two of the neighboring lattice positions are also occupied by styrene monomer units (neglecting end groups), which is a severe restriction for the possible locations of the admantane molecules. The effect of a broader distribution (i) of nearest-neighbor distances can be excluded by the following arguments: The plastic phase of adamantane has a face-centered cubic (fcc) structure,[31] which is a closed-packed structure. Here the adamantane molecules forming the phase have their minimum possible intermolecular distance, which determines the strongest possible dipolar coupling (D_{max}) in the system for the orientation of the dipolar vector parallel to the external magnetic field. Because of the strong orientational dependence of the dipolar interaction, the actual coupling is in general smaller than this maximum coupling and is distributed between D_{max} and $-D_{max}/2$. In the glassy system D_{max} is determined by the minimum possible distance of two adamantane molecules which is the same as above; however, as a result of distortions caused by the irregular structure of the polymer, these distances will be larger than those in the plastic phase. Thus the actual couplings are the same or smaller than in the crystalline system, leading to an equivalent or slower growth of the multiple quantum coherences. This is in contradiction to our experimental findings and a distribution of couplings alone cannot account for the differences in the master curves.

The effects of the shape of the glass-forming polymer molecules (ii) are as follows: When comparing the same concentration of protonated adamantane in the deuterated host, there is a completely random distribution of the protonated

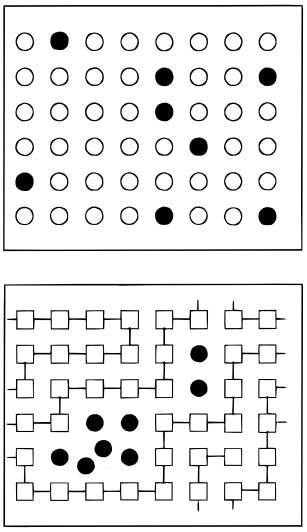

Figure 9. Schematic comparison of the statistical distribution of protonated adamantane (full circles) in deuterated adamantane (open circles, upper panel) and in deuterated polystyrene (open squares, lower panel). The geometrical constraints caused by the chain nature of the polymer are reflected in fluctuations in the pair correlation function of the A-h_{16} molecules.

adamantanes in the crystal, while in the glass there are spatial fluctuations, with adamantane-depleted regions at a polystyrene molecule and adamantane-enriched regions between polystyrene molecules. This model for the coupling is schematically shown in Figure 9 which shows the effective number of coupled guests in the two systems. Consequently, for short coupling times τ, a faster growth of $n(\tau)$ can be expected in the polystyrene matrix, which corresponds to a higher effective adamantane concentration. On the other hand, if we are observing $n(\tau)$ at longer coupling times, the situation is reversed, because then couplings between molecules from different neighborhoods come into play, which are weaker than the average coupling for a purely random distribution of the guest molecule, due to this pseudoclustering of the guest molecules. Thus, for longer coupling times τ, $n(\tau)$ is expected to grow faster for the crystalline system. If we compare the experimental curves of $n(\tau)$ at equal guest concentration, we find these simple predictions in good accord with our data. For short coupling times τ, the cluster size $n(\tau)$ is higher in the polystyrene matrix while for longer values of τ, the curve for the polystyrene matrix lies below the curve of the crystalline system.

These effects are also reflected in the dependence of the homonuclear dipolar line width on the concentration (see Figure 4). As discussed above, the adamantane-enriched regions correspond to a higher effective concentration, which causes a higher contribution of the homonuclear dipolar line width at the same adamantane concentration. For increasing adamantane concentrations this effect will become smaller, and thus a weaker slope of the line width to concentration dependence is expected. This compares well with the curves of the line width as a function of the concentration, which exhibit the discussed behavior.

This has the following consequences for the master curve: Because the scaling was done with the dipolar line width determined from Figure 4, at low coupling times an identical master curve is expected for both systems. However, for long coupling times because of the slower growth in the glassy system the scaled curve will be below the curve of the crystalline system. These predictions are in good accord with the experimental findings.

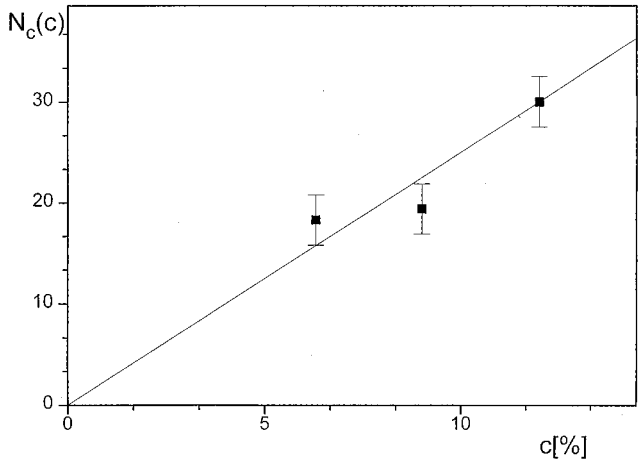

Figure 10. Number of correlated spins as a function of the concentration for a given coupling time $\tau/\tau_c = 24$. The symbols mark the experimental values and the solid line shows an extrapolation to arbitrary concentrations. This curve is used to determine the unknown adamantane concentrations during precipitation.

A quantitative interpretation of our results would require numerical Monte Carlo simulations of the multiple quantum dynamics on a disordered lattice, which are beyond the scope of this article.

4.2. Phase Separation Kinetics of Adamantane in Polystyrene. Mixtures of a polymer and a low molecular weight additive can perform phase separation upon cooling. A recent review of the structure of polymer blends and the characterization of phase separation in such systems is given in ref 12. The temperature dependence of the viscosity of a polymer melt is greater than an Arrhenius dependence, and near the glass transition temperature (T_g) the viscosity reaches a magnitude of the order of 10^{10} P or higher. Due to this high viscosity of the polymer melt such a segregation process may take minutes or hours near T_g. The phase separation process is usually stopped completely when the system is cooled well below T_g. Thus, measuring MQ spectra at room temperature after tempering the system above T_g allows for studying the phase separation as a function of tempering time and temperature. The evolution of the dipolar couplings among different adamantane molecules in the deuterated polymer is used to study the evolution of the segregation process on a molecular scale.

For a quantitative evaluation of the adamantane concentration a calibration curve of the measured cluster size as a function of the concentration of guest molecules is needed. Figure 10 shows the dependence of the measured cluster size as a function of known concentrations of guest molecules in the polystyrene matrix for a fixed coupling time of $\tau/\tau_c = 24$. The result is consistent with a linear dependence through the origin, which is shown by the solid line. This curve is used as a standard for determining the adamantane concentration from the experimentally determined cluster sizes. To study phase separation processes of adamantane guest in the polystyrene matrix the multiple quantum spectra of the 12% sample after tempering the sample at 103 °C for different times were recorded. The sample was rapidly heated by bringing it into contact with a heat bath and at the end of each tempering interval rapidly cooled down to room temperature to stop further phase separation processes. The times for changing the temperature of the sample (order of seconds) were fast compared to the phase separation times and are therefore negligible. The spectra taken after different tempering times using a short coupling time of $\tau/\tau_c = 8$ are shown in Figure 11, and the corresponding spectra for a long coupling time of $\tau/\tau_c = 24$ are shown in Figure 12.

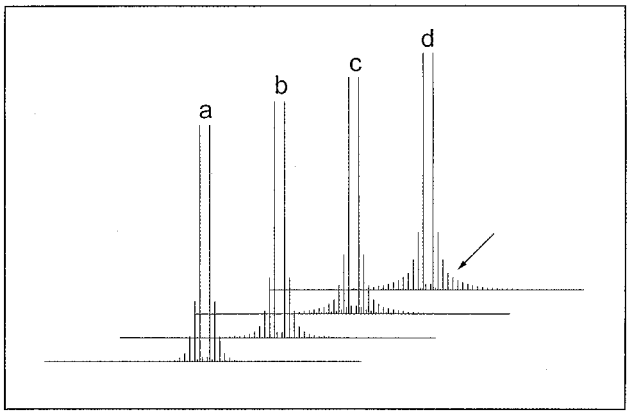

Figure 11. Normalized multiple quantum spectra after four different tempering times (20, 40, 60, 80 min) measured at a short coupling time (8 cycles), where the precipitated and the dissolved adamantane are both visible. Note the increasing precipitation which is visible in the growth of the broad wings of the line for longer temper times marked by the arrow.

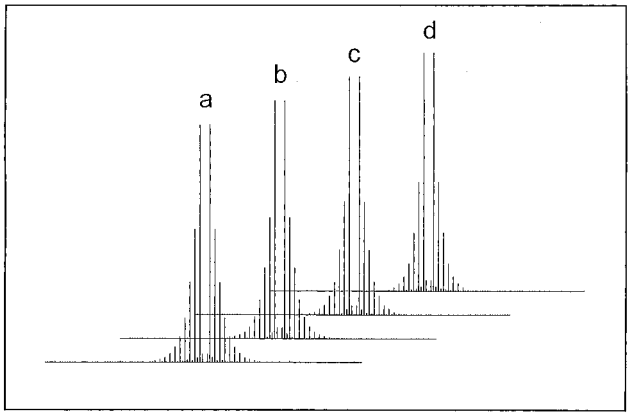

Figure 12. Normalized multiple quantum spectra after the same four different tempering times (20, 40, 60, 80 min) measured at a long coupling time (24 cycles), where only the dissolved adamantane is visible. Note the decrease of the line width for longer temper times, which shows that adamantane leaves the dissolved phase during precipitation.

For $\tau/\tau_c = 8$ the multiple quantum spectra can be decomposed into two components, a rather narrow component with a slightly decreasing width for increasing temper time and a broad component, which is strongly increasing in width and relative intensity for longer temper times. A comparison of the broad component from the spectrum with the longest temper time with the multiple quantum spectrum of pure protonated adamantane at the same coupling time (Figure 13) shows that the broad component is characteristic for regions of pure adamantane. This is strong evidence that the adamantane precipitates during the progress of tempering, leading to a phase separation into a phase of pure admanantane and a phase of residual adamantane dissolved statistically in the matrix. Moreover, the increase in the relative intensity of the wings (Figure 11) shows the increase of the number of adamantane islands in the polystyrene matrix, while the increasing width of the broad components reflects directly the growing size of the single adamantane islands.

This phase separation also affects the spectra recorded with long coupling times ($\tau/\tau = 24$), which selectively reflect the adamantane molecules dissolved in the polymer (Figure 12). Here the decrease of the width of the multiple quantum spectra indicates that the concentration of adamantane dissolved in the polymer is decreasing. Using the calibration curve (Figure 10) the concentration of the adamantane remaining dissolved in the polystyrene host is determined. The result (Figure 14) shows

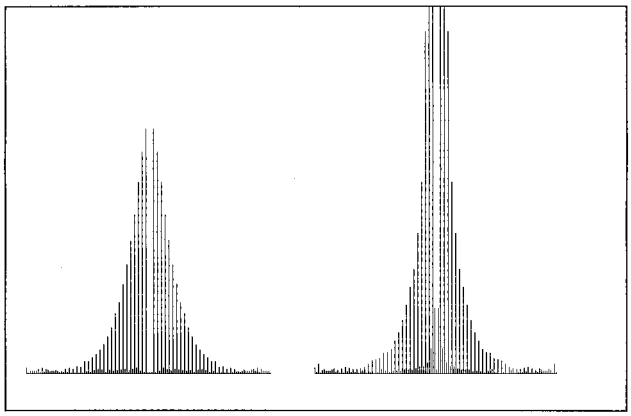

Figure 13. Comparison of the crystalline section of the spectrum with the longest temper time (spectrum d from Figure 9, 80 min) on the right side with the multiple quantum spectrum of pure adamantane (8 cycles, left side). Note that the wings of the two spectra are nearly identical. This shows that crystalline adamantane has precipitated. The differences in the center are caused by the adamantane remaining dissolved in the polystyrene.

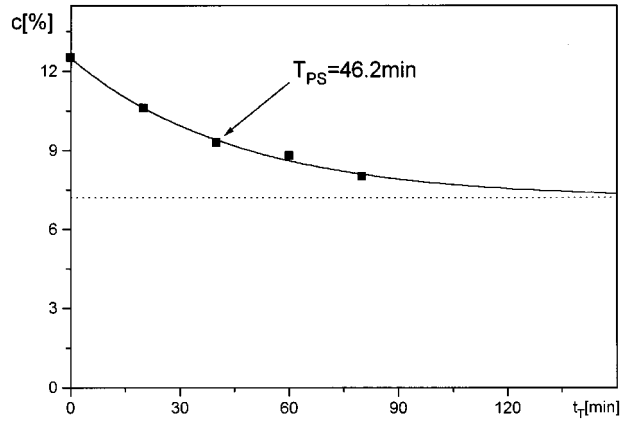

Figure 14. Decay of the adamantane concentration dissolved in the polystyrene matrix as a function of the temper time during the phase separation (T = 130 °C). With a time constant of 47 min the concentration of the adamantane approaches the solution limit of 7% (horizontal line). The solid line marks the result of an exponential fit of the data.

the concentration of adamantane in the polystyrene, $c(t_T)$, as a function of the temper time t_T. In good approximation $c(t_T)$ decreases exponentially (solid line in Figure 14) from the initial value c_0 to the final value of $c_\infty \approx 7\%$ with a time constant of $T_{PS} = 46.2$ min:

$$c(t_T) = c_\infty + (c_0 - c_\infty) \exp\left(-\frac{t_T}{T_{PS}}\right) \qquad (11)$$

It follows that the solution limit of adamantane in polystyrene at $T = 103$ °C is 7%.

5. Summary and Conclusions

Using rf pulses with high B field homogeneity and exact phase setting it has been demonstrated that it is possible to detect large spin clusters of more than 1000 spins in a sample with predominantly intermolecular dipolar couplings and favorable relaxation behavior. This is close to the maximum number of coupled spins detectable by multiple quantum NMR, because relaxation processes impose a sensitivity limit for large values of the coupling time τ necessary for establishing these high coherence orders. In particular, the shape of the growth curves of the multiple quantum coherences can be distorted by

relaxation, as we have found for other systems with less favorable relaxation behavior.

In all dilute systems under study here a concentration-independent master curve of the cluster size $n(\tau)$ as a function of the coupling time τ was obtained by scaling with the square root of the homonuclear dipolar line width $(\Delta\nu)^{1/2}$. The shape of this master curve exhibits characteristic features which can be correlated to the local geometrical structure of the system. For the crystalline isotopically mixed adamantane system the master curve is approximated by a parabolic function (or equivalently well by an exponential of the square root of the coupling time). Thus, for these systems the same master curve is found as for bulk systems known from literature.[11] In contrast, for the glassy polymer system the master curve is given by a linear function where the number of coupled spins $n(\tau)$ is proportional to τ. For short coupling times these differences of the multiple quantum dynamics can be understood by comparing the regular structure of the crystalline system, which ensures a purely statistical distribution of the adamantane guests, with the irregular structure of the polymer where the statistical distribution of the adamantane guests is distorted by the geometrical constraints. For long coupling times, however, two different explanations, which do not necessarily exclude each other, are possible: The differences can be caused either by the same structural difference as above or they can be caused by dynamical processes in the glass forming host polymer. Furthermore, it was shown that multiple quantum NMR allows the study of phase separation processes in binary systems, in particular to investigate the early stages of such processes, which are hardly accessible by other experimental techniques. As an experimental example we have extracted the concentration in each phase of an adamantane/polystyrene mixture undergoing phase separation during tempering at a temperature above T_g. Above the glass transition temperature adamantane-enriched regions and adamantane-depleted regions develop, until for long temper times neat adamantane precipitates. This phase separation was monitored by observing both the appearance and growth of the adamantane enriched phase in the multiple quantum spectra recorded with short coupling times and the depletion of the adamantane in the polymer phase in the spectra recorded with long coupling times. These processes continue until the solution limit of adamantane in polystyrene is reached.

By measuring the complete τ dependence of the MQ spectra, the differences in the master curve of the crystalline versus the glassy system can be exploited to map out the changes of the pair correlation function of the guest molecules in the polystyrene during the phase separation process.

Acknowledgment. We thank Prof. U. Haeberlen (MPI Heidelberg) for his donation of an NMR coil with high rf homogeneity. This work was supported by the Deutsche Forschungsgemeinschaft.

References and Notes

(1) Yen, Y.-S.; Pines, A. *J. Chem. Phys.* **1983**, *78*, 3579.
(2) Baum, J.; Gleason, K. K.; Pines, A.; Garroway, A. N.; Reimer, J. A. *Phys. Rev. Lett.* **1986**, *56*, 1377.
(3) Baum, J.; Pines, A. *J. Am. Chem. Soc.* **1986**, *108*, 7447.
(4) Drobny, G.; Pines, A.; Sinton, S.; Weitekamp, D. P.; Wemmer, D. *Faraday Symp. Chem. Soc.* **1979**, *13*, 49.
(5) Munowitz, M.; Pines, A. *Science* **1986**, *233*, 525.
(6) Weitekamp, D. P. *Adv. Magn. Reson.* **1983**, *11*, 111.
(7) Bodenhausen, G. *Prog. NMR Spectrosc.* **1981**, *14*, 137.
(8) Munowitz, M. *Coherence and NMR*; Wiley: New York, 1988, Chapter 6.
(9) Lacelle, S. *Adv. Magn. Opt. Reson.* **1991**, *16*, 173.
(10) Amoureux, J. P.; Bee, M.; Virlet, J. *Mol. Phys.* **1980**, *41*, 313.
(11) Scruggs, B. E.; Gleason, K. *J. Magn. Reson.* **1992**, *99*, 149. Levy, D. H.; Gleason, K. K. *J. Phys. Chem.* **1992**, *96*, 8125.
(12) Hashimoto, T. In *Materials Science and Technology*; Cahn, R. W., Haasen, P., Kramer, E. J., Eds.; VCH: Weinheim, Germany 1993; p 12.
(13) Hashimoto, T.; Itakura, M.; Hasegawa, H. *J. Chem. Phys.* **1986**, *85*, 6118.
(14) Strobl, G. R. *Macromolecules* **1985**, *18*, 558.
(15) Schwahn, D.; Hahn, K.; Streib, J.; Srpinger, T. *J. Chem. Phys.* **1990**, *93*, 8383.
(16) Wang, P. K.; Slichter, C. P.; Sinfeldt, J. H. *Phys. Rev. Lett.* **1984**, *53*, 82.
(17) Pines, A. *Proc. 100th School Phys. Enrico Fermi* **1988**, 43.
(18) Shykind, D. N.; Baum, J.; Liu, S.-B.; Pines, A.; Garroway, A. N. *J. Magn. Reson.* **1988**, *76*, 149.
(19) Emid, S. *Physica B* **1985**, *128*, 79.
(20) Warren, W.; Weitekamp, D. P.; Pines, A. *J. Chem. Phys.* **1980**, *73*, 2084.
(21) Slichter, A. *Principles of Magnetic Resonance*, 3rd ed.; Springer-Verlag: Berlin, 1990.
(22) Rhim, W.-K.; Burum, D. P.; Elleman, D. D. *Phys. Rev. Lett.* **1976**, *37*, 1764.
(23) Munowitz, M. *Mol. Phys.* **1990**, *71*, 959.
(24) Munowitz, M.; Pines, A.; Mehring, M. *J. Chem. Phys.* **1987**, *86*, 3172.
(25) Abragam, A. *Principles of Nuclear Magnetism*; Clarendon Press: Oxford, U.K., 1961; p 126.
(26) Mehring, M. *High Resolution NMR Spectroscopy in Solids*; Springer-Verlag: New York, 1983; p 208.
(27) Idziak, S.; Haeberlen, U. *J. Magn. Reson.* **1982**, *50*, 281.
(28) Baum, J.; Munowitz, M.; Garroway, A. N.; Pines, A. *J. Chem. Phys.* **1985**, *83*, 2015.
(29) Murdoch, J. B.; Warren, W. S.; Weitekamp, D. P.; Pines, A. *J. Magn. Reson.* **1984**, *60*, 205.
(30) Scruggs, B. E.; Gleason, K. *Chem. Phys.* **1992**, *166*, 367.
(31) Amoureux, J. P.; Bee, M.; Damien, J. C. *Acta Crystrallogr.* **1980**, *B36*, 2633.
(32) Gleason, K. K.; Lathrop, D. A.; Zhang, L. *35th ENC Asilomar* **1994**, 78.
(33) Roessler, E. *Habilitationsschrift* **1992**.

JP960963D